Self-assembly of magnetically interacting cubes by a turbulent fluid flow

Filip Ilievski,[1] Madhav Mani,[2] George M. Whitesides,[1] and Michael P. Brenner[2]
[1]*Department of Chemistry, Harvard University, Cambridge, Massachusetts 02138, USA*
[2]*School of Engineering and Applied Sciences, Harvard University, Cambridge, Massachusetts 02138, USA*
(Received 22 September 2010; published 5 January 2011)

Previous work has demonstrated that combining mechanical vibration with magnetic interactions can result in the self-assembly of complex structures, albeit at low yield. Here we introduce a system where the yield of self-assembled structures is quantitatively predicted by a theoretical analysis. Millimeter-sized magnetic blocks, designed to form chains as their minimal energy state, are placed in a turbulent fluid flow. The distribution of chain lengths that form is quantitatively consistent with predictions, showing that the chain length distribution coincides with that of monomers or polymers in a thermal bath, with the turbulence strength parametrizing the effective temperature.

DOI: 10.1103/PhysRevE.83.017301 PACS number(s): 82.70.Dd, 45.70.−n

Self-assembly promises a new paradigm for manufacturing small devices: instead of piece-by-piece manufacturing, structures could spontaneously assemble from individual components into functional devices [1–5]. Enabling this technology requires understanding how to design parts, and protocols for their assembly, such that structures assemble with high yield. Examples from physics have abundantly shown that collections of identical parts, under either equilibrium [6,7] or nonequilibrium conditions [8], allow many different structures to form, each in low yield. The fundamental question is to understand how to choose the parts, component and the recipe for self-assembly, to maximize the yield of a prespecified product. To date, perhaps the most versatile strategy for self-assembly that has been employed uses DNA [9,10]. This work includes the demonstrations of DNA assembly of complex two-dimensional shapes [9] and nontrivial dynamic structures such as an autonomous walker [10,11].

DNA-based self-asssembly brings great variability to the generation of molecular assemblies with unexpectedly complex geometries, but it has not, so far, suggested strategies for assembly of functional structures. Practical materials require the development of methods for assembling structures other than DNA, or those based on DNA at length scales ranging from microscopic to macroscopic. Whereas submicron assembly can be driven by thermal fluctuations, macroscopic (i.e., millimeter-sized) assembly cannot; in this range of sizes, assembly requires inputting energy. A common method for assembling macroscopic objects is vibration. For example, Boncheva *et al.* [1] showed that shaking a polydimethylsiloxane (PDMS) sheet embedded with small magnets allowed the sheet to fold into a closed structure; Rothemund showed that shaking floating particles [12], with hydrophobic and hydrophilic patches, could facilitate the formation of dense prespecified arrays. But, in both cases, the dynamics leads to structures that do not have the desired pattern; for example, the yield for folding sheets into closed surfaces is in practice quite small; others, such as Jacobs *et al.* [13], report high-yield self-assembled structures based on capillary interactions in low-melting-temperature solders.

For vibration-based self-assembly to be a viable manufacturing strategy, we must design structures and strategies for agitation that allow self-assembly to proceed to a desired state in high yield. The first step in developing a design strategy is the ability to predict yield quantitatively. With an accurate quantitative model for yield, we can design systems (component parts and vibration strategy) where the yield is maximized. Heretofore, studies of vibration-based self-assembly have been qualitative, with no underlying theoretical basis.

The goal of this Brief Report is therefore to introduce a system in which the self-assembly yield can be quantitatively controlled and compared with theoretical predictions. To this end, we have designed a system in which millimeter-sized magnetic blocks assemble into chains in a turbulent fluid flow. The statistics of turbulent fluid flows have been well characterized [14–16], leading to a stochastic forcing of the particles; this is precisely analogous to a thermal bath, with the effective temperature depending on the strength of the turbulence. The distribution of chain lengths of the magnetic blocks can be controlled by changing either the strength of the turbulence or the magnetic binding energy. The observed distributions are well described by a theoretical model, which is based on a first-principles description of the mechanics of particles in a turbulent flow.

The magnetic blocks are PDMS cubes (side length 1 cm), with small disk-shaped magnets (1/8 in. diameter and 1/32 in. thickness, made out of NdFeB) embedded in the center of one face of the cube, with the north pole facing outward. A 1/4 in. × 1/4 in. × 1/8 in. square prism of soft ferromagnetic NiCu alloy is embedded on the opposite face [Fig. 1(a)]. Two such cubes interact by lining up the permanent magnet with NiCu; all other permutations are not energetically favorable, since two faces with identical magnets repel, and there is no significant interaction between two faces with NiCu. NiCu was selected because of its easily accessible Curie temperature, or the temperature where the material turns from ferromagnetic to paramagnetic. We measured the low Curie temperature for this alloy to be $T_{\text{Curie}} = 165\,^{\circ}\text{C}$; this value of T_{Curie} is such that we can tune the interaction energy between the magnets by changing the temperature of the system. To tune the vibrations, we place N cubes in a closed container (diameter 8 cm and height 10 cm) filled with water with 0.3 M CsCl (for matching the density of the cubes) and 10 mM Triton-X 100 (to minimize bubble formation on agitation). The jar is then attached to a 60-cm-diam disk which is rotated at a frequency f between 9 and 80 rpm [Fig. 1(b)]. Changing the rotation

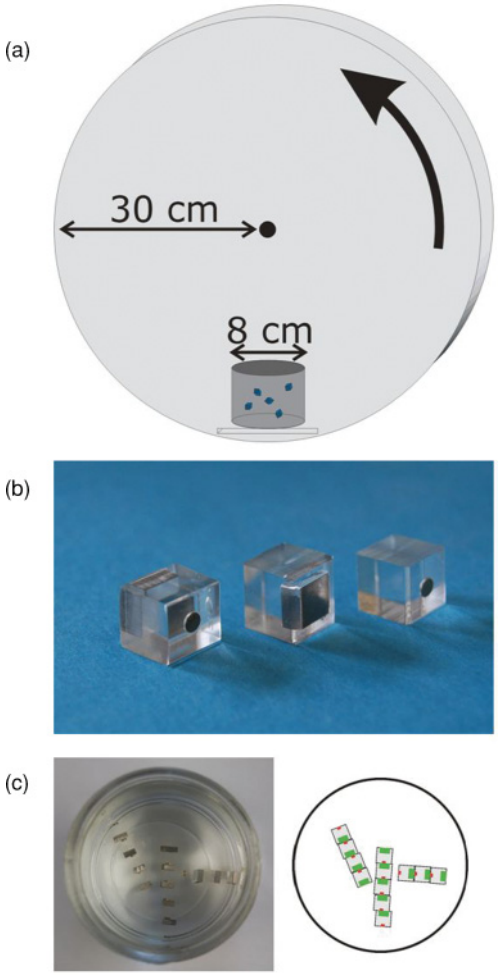

FIG. 1. (Color online) (a) Schematic sketch of the experiment. N cubes are placed in a closed container, which is then attached to a rotating disk that generates a turbulent flow. (b) Polydimethylsiloxane blocks with small embedded disk-shaped magnets and prism-shaped NiCu pieces. (c) Agitation in a turbulent flow causes the blocks to form chains; green (dark gray), NiCu pieces; red (light gray), magnets.

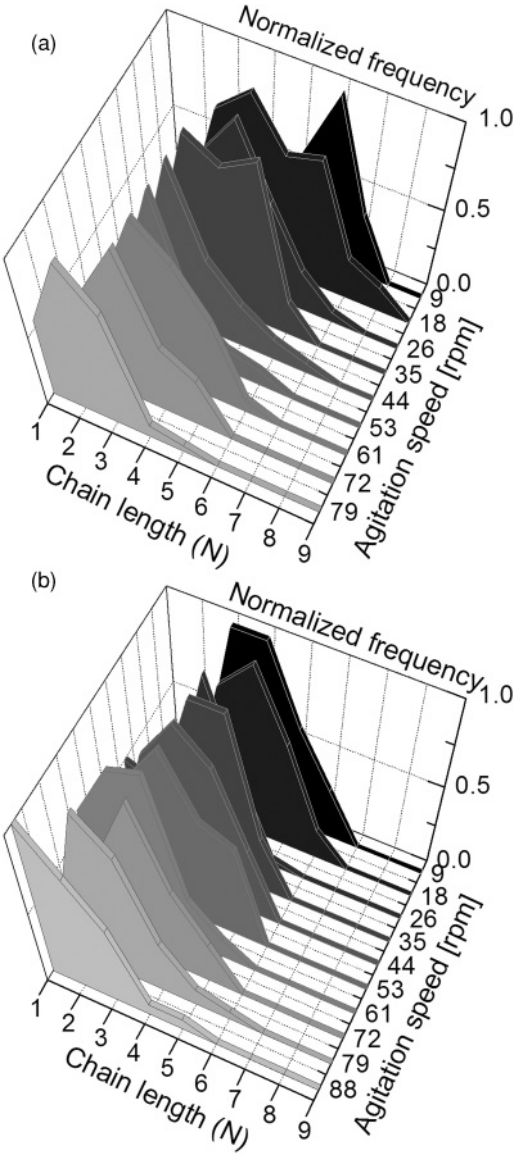

FIG. 2. Histogram of the distribution of chain lengths measured in the experiment, for a range of different rotation rates, and both (a) room temperature and (b) $T = 80\,^{\circ}$C. Changing the temperature shifts the strength of the magnetic interaction. The peak of the distribution shifts as a function of both temperature and rotation rate.

frequency allows a continuous tuning of the strength of the turbulence.

In a typical experiment, we begin with $N = 12$ dissociated monomers, and we rotate the jar for 50 full rotations. We then examine the distributions of chain lengths that form [Fig. 1(c)]. The chains are manually disassembled into monomers before repeating the experiment. Figure 2(a) shows the results of the experiment at room temperature. For each rotation frequency f, a range of different chain lengths can form, though there is a chain length N^* for which the yield is maximal. N^* decreases with increasing f. The distribution is broad peaked, so the yield at the maximum N is rather low, of order 15%–20%. By changing the temperature to $T = 80^{\circ}$C, we can tune the strength of the magnetic interaction and, hence, shift the distribution [Fig. 2(b)].

We now turn to a theoretical description of the assembly process. The rotation of the cylinder produces a time-dependent flow inside the jar; the monomers move both from their interactions with each other and from the turbulence. The translational equation of motion for the center of mass of the ith monomer is thus

$$m_p \frac{d^2 x_i}{dt^2} = c_D \frac{dx_i}{dt} - \nabla V(X_i) + \xi(t). \tag{1}$$

The inertia of the particle, with mass m_p, is dissipated in proportion to the velocity of the particle, where c_D is the drag coefficient. The particles interact with each other through a magnetic potential, $V(x_i) = \sum_{i \neq j} U(|x_i - x_j|)$, which sums the magnetic interaction $U(\eta)$ set up by the surrounding particles. $\xi(t)$ represents the agitation the flow provides to the particle.

The quantitative values of both the drag coefficient c_D and the turbulent forcing $\xi(t)$ depend on the size of the particles relative to the turbulent eddies in the fluid flow. A typical

eddy size is the Kolmogorov microscale, ℓ_η, the length scale at which the local Reynolds number is equal to unity; in the present experiments, this is $\ell_\eta \approx 10^{-3}$ cm, far smaller than the size of the cube, $d_p \approx 1$ cm. This implies that the drag on the particle is dominated by the viscous stresses exerted on the particles by the eddies of competing size. Phenomenological characterizations of this drag [17] estimate the drag coefficient to be $c_D = 24\pi\mu d_p(1 + 0.1315\mathrm{Re}_p^n)$, where $\mathrm{Re}_p = (d_p/\ell_\eta)^{4/3}$ and $n = 0.82 - 0.05\log_{10}\mathrm{Re}_p$.

To understand the turbulent forcing $\xi(t)$, note that the typical deceleration time scale for the particle (m_p/c_D) is $\approx$25 times slower than the turnover time scale of turbulent eddies [14,17]. Thus, on the typical time scales of particle motion, the fluid forcing behaves as a time-uncorrelated process [18–20]. The central limit theorem therefore implies that the fluid forcing is temporally uncorrelated, Gaussian, and with zero mean. Hence, we have $\langle\xi(t)\rangle = 0$ and $\langle\xi(t')\xi(t'')\rangle = 2q\delta(t' - t'')$, which implies a particle diffusion constant to be $D = m^2q/2c_D^2$. The noise strength q can be estimated by considering that the viscous stress exerted by an eddy of size d_p on the particle is $\tau \sim \mu\langle\delta u(d_p)^2\rangle^{1/2}/d_p$, where $\langle\delta u(d_p)^2\rangle^{1/2}$ is the typical velocity of an eddy of size d_p. This quantity is referred to as the second-order structure function of a turbulent flow, and several investigators [16] have confirmed the scaling laws predicted by Kolmogorov's theory. We can hence estimate $q \approx 0.147\ (\mathrm{cm/s^2})^2$ and $c_D/m \approx 5\ \mathrm{s}^{-1}$ for the current system.

With these assumptions, Eq. (1) is a classical Langevin equation [21]. The flow configuration is therefore identical to a set of interacting particles in a thermal bath, with an effective temperature $k_BT_{\mathrm{eff}} = c_DD$. The stationary probability distribution can be obtained by solving the associated Fokker-Planck equation; this stationary distribution is simply given by the Boltzmann distribution for the interacting particles, with the temperature T_{eff}. The present problem is analogous to finding the probability distribution of the distribution P_N of chain lengths of linear monomers of length N in a thermal bath, a classical problem of polymer physics [22]. The probability distribution requires computing the partition function $\Sigma_N Q_N$ for linear aggregates of size N; this decomposes into its translational (q_t), rotational (q_r), vibrational (q_v), and bulk terms

$$Q_N = q_t^{(N)}q_r^{(N)}(q_v e^{-V^*/k_BT_{\mathrm{eff}}})^N, \tag{2}$$

where V^* is the binding energy of two magnets to each other.

Following [22], we can evaluate the various partition functions: the translational partition function is given by $q_t \sim (Nmk_BT_{\mathrm{eff}})^{3/2}$, whereas the rotational partition function for a rod of length $L = N\ell$, where ℓ is the dimension of each block, is given by $q_r \sim (I_{AN}k_BT_{\mathrm{eff}})^{1/2}(I_{BN}k_BT_{\mathrm{eff}})$, where I_{AN} and I_{BN} are the moments of inertia for rotating a linear aggregate of length N around its long axis and perpendicular axes, respectively. These are thus given by $I_{AN} = m\ell^2N/8$ and $I_{BN} \approx mNL^2/48 = mN^3\ell^2/48$, respectively. Putting this together, we have that $Q_N \sim N^5x^N$, where the factor $x = e^{-V^*/k_BT_{\mathrm{eff}}}$. This therefore implies that the probability distribution is given by

$$\frac{P}{P_{N_m}} = \left[\frac{N}{N_m}\exp\left(1 - \frac{N}{N_m}\right)\right]^5, \tag{3}$$

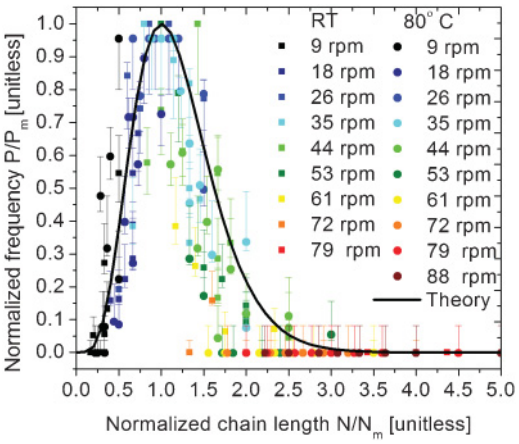

FIG. 3. (Color online) Comparison of theoretical prediction and normalized experimental results: symbols represent data from aggregates at room temperature and 80 °C, and the colors represent different rotation speeds. The solid line is the theoretical prediction [Eq. (3)]. The error bars are statistical [23].

where the most probable configuration occurs at chain length N_m:

$$N_m \sim -\frac{5k_BT_{\mathrm{eff}}}{V^*}. \tag{4}$$

This theoretical description makes a number of explicit predictions that can be tested in experiments. First, the shape of the probability distribution depends on a single parameter N_m; if we take the measured distributions shown in Fig. 2 and rescale the chain lengths by N_m, and rescale the probabilities by the measured $P(N_m)$, the distributions should collapse onto a single curve. Figure 3 shows this collapse, compared with the theoretical prediction for the shape of the distribution given in Eq. (3). The different colors in the figure represent different rotation speeds, whereas the different shapes represent two different temperatures (magnetic binding strengths). The error bars on the data points correspond to statistical sampling error [23].

A second prediction of the theory is that the peak position N_m should decrease linearly with the angular velocity of the rotation and depends inversely on the magnetic interaction energy V^* between the monomers. The experiments reported in Fig. 2 vary both f and V^*; changing the temperature from 21°C to 80 °C roughly halves V^*. Figure 4 confirms both predicted relationships: the linear dependence on ω and the predicted change in this relationship following an increase in the real temperature.

To summarize, we have demonstrated that a turbulent flow can be used to create a well-controlled effective thermal bath for a mesoscopic self-assembling system. This allows the design of an experimental system where the assembly yield can be well controlled and predicted by theoretical analysis. Changing both the strength of the turbulence and the binding energy of the magnets causes changes in the measured probability distributions of the chain lengths that are well captured by the theory. While the theory explained here predicts well the behavior of the system, it should be noted that Eq. (3) is valid in the dilute limit; further refinements, such as hydrodynamic effects between cubes, have been ignored

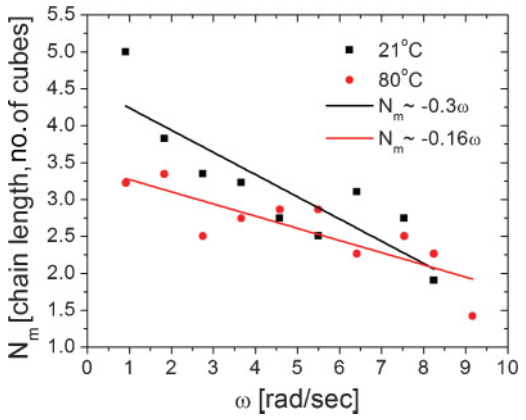

FIG. 4. (Color online) Peak position, N_m, vs angular velocity of the jar, ω: squares and circles represent data from experiments conducted at room temperature and 80 °C, respectively. The lines represent a best fit through the data with the gradient stated in the legend. This figure provides evidence for the predicted linear relationship between N_m and ω and the dependence on the interaction energy.

since these effects are smaller than the magnetic interactions between the cubes when they are in close proximity to each other.

This work leads to several points that are significant for mesoscale self-assembly: The ability to create a controlled white noise source where the assembled yield can be predicted leads to the possibility of *a priori* designing the interactions between the structures (by tuning the strengths of the magnets or their positions) to maximize the yield of the desired structure. More generally, there is tremendous opportunity for using flow fields—turbulent or not—for controlling the assembly of mesoscopic objects. While this idea is in its infancy, the simple method seems to present opportunity for controlling and designing self-assembling systems on intermediate length scales. Another intriguing possibility is the use of chaotic advection in planar or microfluidic flows for creating effective temperature fields for millimeter-sized objects. The advantage here is that in addition to the random component there is also a mean flow; one could imagine creating a multistaged "factory" for creating complex structures. A major challenge is to use this methodology to design useful structures at the millimeter scale, where the flow characteristics and interactions are chosen to maximize yield.

This research was supported by DARPA under Contract No. BAA07-21, the National Science Foundation through the Harvard MRSEC, and the Kavli Institute for Bionano Science and Technology at Harvard University.

[1] M. Boncheva, S. A. Andreev, L. Mahadevan, A. Winkleman, D. R. Reichman, M. G. Prentiss, S. Whitesides, and G. M. Whitesides, Proc. Natl. Acad. Sci. USA **102**, 3924 (2005).
[2] G. M. Whitesides and M. Boncheva, Proc. Natl. Acad. Sci. USA **99**, 4769 (2002).
[3] G. M. Whitesides and B. Grzybowski, Science **295**, 2418 (2002).
[4] G. M. Whitesides, Chimia **59**, 65 (2005).
[5] M. Boncheva and G. M. Whitesides, MRS Bull. **30**, 736 (2005).
[6] G. Meng, N. Arkus, M. Brenner, and V. Manoharan, Science **327**, 560 (2010).
[7] M. Fialkowski, A. Bitner, and B. Grzybowski, Nat. Mater. **4**, 93 (2005).
[8] T. A. Witten and L. M. Sanders, Phys. Rev. Lett. **47**, 1400 (1981).
[9] P. W. K. Rothemund, Nature (London) **440**, 297 (2006).
[10] S. Douglas, H. Dietz, T. Liedl, B. Hogberg, F. Graf, and W. Shih, Nature (London) **459**, 414 (2009).
[11] P. Yin, H. Yan, X. G. Daniell, A. J. Turbereld, and J. H. Reif, Angew. Chem. Int. Ed. **43**, 4906 (2004).
[12] P. W. Rothemund, Proc. Natl. Acad. Sci. USA **97**, 984 (2000).
[13] H. O. Jacobs, A. R. Tao, A. Schwartz, D. H. Gracias, and G. M. Whitesides, Science **296**, 323 (2002).
[14] Z. Warhaft, Annu. Rev. Fluid Mech. **32**, 203 (2000).
[15] U. Frisch, *Turbulence: The Legacy of A. N. Kolmogorov* (Cambridge University, Cambridge, UK, 1995).
[16] S. B. Pope, *Turbulent Flows* (Cambridge University, Cambridge, UK, 2000).
[17] H. Xu and E. Bodenschatz, Physica D **237**, 2095 (2008).
[18] J. Bec, L. Biferale, M. Cencini, A. Lanotte, S. Musacchio, and F. Toschi, Phys. Rev. Lett. **98**, 084502 (2007).
[19] H. Homann and J. Bec, J. Fluid Mech. **551**, 81 (2009).
[20] J. Bec, M. Cencini, and R. Hillerbrand, Physica D **226**, 11 (2007).
[21] N. van Kampen, *Stochastic Processes in Physics and Chemistry* (Elsevier, Amsterdam, 1981).
[22] T. L. Hill, *Linear Aggregation Theory in Cell Biology* (Springer-Verlag, New York, 1987).
[23] R. G. Newcombe, Stat. Med. **17**, 875 (1998).